# The core–mantle boundary layer and deep Earth dynamics

Thorne Lay, Quentin Williams & Edward J. Garnero

**Recent seismological work has revealed new structures in the boundary layer between the Earth's core and mantle that are altering and expanding perspectives of the role this region plays in both core and mantle dynamics. Clear challenges for future research in seismological, experimental, theoretical and computational geophysics have emerged, holding the key to understanding both this dynamic system and geological phenomena observed at the Earth's surface.**



The Earth acquired its primary layered structure—consisting of a molten metallic alloy core overlain by a thick shell of silicates and oxides—very early in its history, and the region near the core–mantle boundary (CMB) surface has undoubtedly played a significant role in both the core and mantle dynamic systems throughout their subsequent 4.5-Gyr evolution. The CMB has a density contrast exceeding that found at the surface of the Earth, has contrasts in viscosity and physical state comparable to those at the ocean floor, and has much hotter ambient temperatures than found near the surface[1,2]. These factors, together with the requirement that significant heat be flowing from the core into the mantle in order to sustain the geodynamo (the core magnetohydrodynamic flow regime that produces the Earth's magnetic field), provide the basis for the conventional view that a significant thermal boundary layer exists at the base of the mantle, with a temperature contrast of 1,000 ± 500 K (refs 2–4). With ambient temperatures averaging around 3,000 K, this hot thermal boundary layer is a likely source of boundary-layer instabilities, and it has been speculated that upwelling thermal plumes ascend from the CMB to produce surface hotspot volcanism such as at Hawaii and Iceland, transporting about 10–15% of the surface heat flux[5–7]. The large CMB density contrast favours a mantle-side accumulation of chemical heterogeneities derived from initial and continuing chemical differentiation of the mantle, possibly including downwelling subducted slabs of former oceanic lithosphere; distinctive chemical signatures of these heterogeneities may eventually be entrained into thermal plumes, resulting in unique hotspot chemistry[8,9]. There may also be a core-side chemical and thermal boundary layer, but the low seismic velocities and molten state of the core make it much harder to analyse any structure in the outermost core[2].

In the past decade, seismic tomography has provided steadily improving images of deep mantle elastic velocity heterogeneity, revealing the presence of significant large-scale (>2,000 km) patterns of coherent high- and low-velocity regions at all depths[10–12], with enhanced lateral variations in the lowermost 300 km. Attributing the seismological variations to lateral thermal and chemical heterogeneity in the boundary layer suggests several mechanisms of coupling between the core and mantle, influencing the core flow regime as well as irregularities in rotation of the planet[2,13–15]. An experimental demonstration that chemical reactions may be continuing between the core and mantle has raised the possibility of electromagnetic coupling across the boundary[16,17]. These considerations assign possible importance to the CMB layer for dynamic processes throughout the planet (including an intimate relationship to surface structures), yet the precise role of the CMB region remains a topic of vigorous research and debate requiring improved resolution of the structure and processes operating there.

Several recent seismological discoveries have revealed new attributes of the mantle-side boundary layer overlying the CMB. The lowermost 200 km of the mantle (known as the D″ region) has long been characterized by seismologists as distinctive in its properties from the overlying deep mantle. Numerous studies have revealed the presence of intermittent stratification of the D″ region in many areas, with 1.5–3% velocity discontinuities for both compressional (P) and shear (S) waves at depths of 150–300 km above the CMB[18–21]; studies have also shown the presence of laterally varying shear-wave anisotropy (birefringence that splits the S waves into orthogonal polarizations that travel with different velocities owing to organized mineralogical or petrographical fabrics) in the D″ region that is, at least sometimes, related to the discontinuity structure[22–26]. Both observations lack satisfactory explanations in terms of current understanding of thermal and

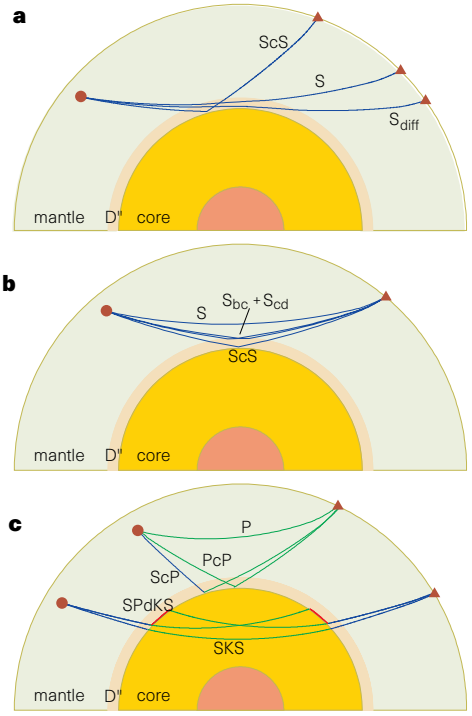


**Figure 1** Seismic-wave ray-paths from a deep focus source (circle) to a receiver (triangle) for phases that have been extensively used to image the velocity structure of the deep mantle. **a**, Core-grazing phases such as the reflection ScS, direct S near 90°, and diffracted S ($S_{diff}$) in the shadow zone. These have P-wave counterparts. Grazing waves provide sensitivity to lateral heterogeneity and anisotropy in the D″ region. **b**, D″ triplication phases, including reflections ($S_{bc}$) and refractions ($S_{cd}$) from a velocity discontinuity. These have P-wave counterparts. Triplications constrain the depth and strength of any discontinuities. **c**, Phases used to study the ULVZ include short-period reflections (PcP) and conversions (ScP), as well as the long-period SKS phase and its associated SPdKS phase (involving P energy diffracted along the core).

mineralogical structure of the deep mantle. A newly discovered laterally varying ultra-low-velocity layer in the lowermost few tens of kilometres of the mantle[27–29] is also challenging the conventional view, as the magnitude of the velocity drop (10% or more reductions in both P and S velocities) is so large that it probably involves partial melting of the mantle, with attendant broad implications for chemical reactions, heat transport, and boundary-layer dynamics[29]. Together with the latest generation of high-spatial-resolution seismic tomography images[30,31], these seismic observations and their spatial systematics raise many questions about primary processes in the CMB boundary layer that define challenging research frontiers for experimental and computational geophysics. The present state of knowledge about the CMB region parallels that of the lithospheric boundary layer in the early 1960s, at the dawn of the plate-tectonics revolution. It is reasonable to expect that a concerted effort to quantify the deep boundary layer processes will achieve large advances in our understanding of the dynamic Earth system.

## Seismological discoveries

The elastic velocity structure of the lowermost mantle has been studied by seismologists for decades[32], yet an important new discovery of some fundamental aspect of the structure in the D″ region has occurred every few years. Although traditional arrival-time analysis procedures for seismic P and S waves continue to lie at the heart of the increasing resolution of seismic tomography models, detailed analysis of waveforms for a variety of secondary phases has played a larger role in revealing high-resolution details of the boundary-layer structure.

Figure 1 illustrates some of the ray paths associated with seismic phases that provide information about the deep mantle structure. P and S waves that graze the D″ region (Fig. 1a), either reflecting off of the core (PcP, ScS) or diffracting along it ($P_{diff}$, $S_{diff}$) have been studied for decades, but recent analysis procedures which account for shallow mantle effects are revealing coherent large-scale patterns that augment those detected by travel-time tomography[33]. Commonly, differential anomalies such as ScS–S arrival times are used to help isolate lower-mantle contributions. The discovery in the early 1980s of a deep-mantle shear-wave reflector several hundred kilometres above the CMB[34] introduced the analysis of reflections and refractions ($S_{bc}$ and $S_{cd}$ in Fig. 1b, and their P-wave counterparts), which are used to map the lateral extent of localized stratification and its depth and material property contrasts. Core-grazing and core-reflected S waves can also be analysed for any shear-wave splitting associated with anisotropic structure near the base of the mantle, although shallow mantle effects need to be accounted for carefully. For examining the seismic properties within tens of kilometres of the CMB, the optimal seismic waves are short-period P reflections (PcP) and S to P conversions (ScP), as well as longer-period S waves that convert at the CMB, transmitting through or diffracting along the CMB as P waves, before they travel back to the surface as S waves (SKS and SPdKS phases in Fig. 1c). PKP phases and their scattered precursors also provide critical information about small-scale structures in D″.

In all cases, the recent availability of large data sets of digital short-period or broadband data from global instrument deployments and global data centres has been critical to the effort to study the deep mantle structure. Based on detailed waveform analysis of the phases mentioned above, constrained by the spatial coverage intrinsic to earthquake and recording-station distributions, recent seismological efforts have mapped out extensive regions of D″ properties that were not even recognized to exist 15 years ago.

## D″ ultra-low-velocity layer

The recently discovered low-velocity layer at the base of the mantle is 5–40 km thick, and has P- and S-wave velocity reductions exceeding 10% (refs 27–29, 35, 36). These velocity variations are much greater than those suggested by travel-time tomography, and this structure is referred to as an ultra-low-velocity zone (ULVZ). The ULVZ is convincingly revealed by delayed and amplified SPdKS phases (relative to SKS) and by precursors to PcP, and has thus far been mapped with the Fresnel-zone (region of coherent wave interaction) coverage shown in Fig. 2a. Although many earlier studies proposed strong velocity decreases in the lowermost mantle from analysis of reflected and diffracted waves, only the recent work provides compelling evidence for the thin basal structure, as well as documenting its lateral variations. Extensive regions of the ULVZ are found beneath the central Pacific Ocean, Alaska, Iceland and Africa. Other areas, indicated in Fig. 2a, have been examined and do not show evidence for this structure, suggesting either that it is not present or that it is thinner than a few kilometres in depth extent, in which case it may be seismically invisible to present methods. In areas such as the central Pacific, the ULVZ shows significant lateral variations in thickness and/or depth extent[37]. Fluctuations in the data indicate that there is substantial sub-Fresnel-zone (that is, unresolved small-scale) structure in the ULVZ, with it being possible that there are localized

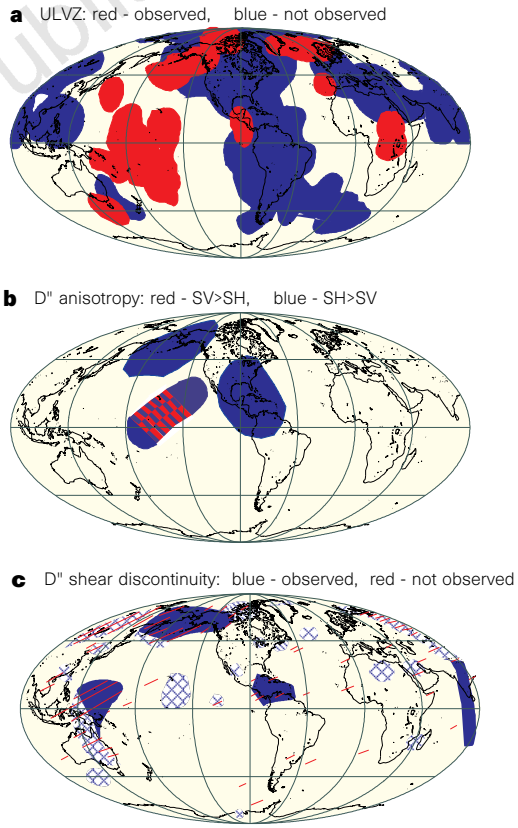


**Figure 2** Mollewide projections summarizing spatial patterns of recently determined seismological characteristics of the CMB boundary layer. **a**, Regions with detectable ultra-low-velocity zone (ULVZ) structure are shown in red, and sampled regions that lack evidence of any ULVZ are shown in blue[29]. **b**, Regions with shear-wave anisotropy in D″ are shown[26]. Transverse isotropy, caused by horizontal layers with strong velocity contrasts (as indicated schematically) or by hexagonally symmetric minerals with aligned vertical symmetry axes, could account for SH waves traveling faster than SV waves in these regions. The central Pacific region has a mix of no anisotropy and general anisotropy (possibly triclinic, or hexagonal symmetric minerals with variably orientated symmetry axes, or lamellae with variable orientation) with relatively small lateral coherence. **c**, Regions with shear-wave discontinuities near the top of the D″ layer. Several regions show large-scale coherence (solid blue), with mixed areas lacking extra reflections (red stripes), while in some areas the reflection from D″ is highly variable and intermittent (cross-hatched)[21].

pockets of very acute heterogeneity rather than any type of uniform layer.

Most seismic observations of the ULVZ are directly sensitive to the P-wave velocity decrease, with there being some sensitivity to very large (>20%) S-wave velocity decreases or density increases[29]. Nonetheless, there is some evidence favouring shear-wave velocity decreases up to three times as strong as the P-wave velocity decrease[35,36]. The velocity contrasts (the sharpness is not yet well resolved, but is probably less than 5 km) associated with this feature are greater than for any of the main transition-zone discontinuities, and are of the order of those associated with contrasts between subducted slabs and overlying zones of partial melt, or shallow heterogeneities in magma chambers beneath active rifting structures such as mid-ocean ridges. The acute velocity heterogeneity of the ULVZ is a likely source of strong scattering of short-period phases that has long been associated with short-wavelength heterogeneity in D″[38,39].

## D″ anisotropy

Analysis of the polarization of shear waves that graze the D″ region has demonstrated the existence of shear-wave anisotropy for certain paths: that is an unexpected discovery given that there is almost no evidence for anisotropic effects on body waves for paths traversing the lower mantle above the D″ region[40,41]. For paths sampling beneath circum-Pacific regions, the observed shear-wave splitting is such that horizontally polarized SH waves arrive ahead of vertically polarized SV waves. Although the data do not fully constrain the geometry of the anisotropy (there is usually very limited azimuthal sampling of any given region), the observations are consistent with transmission through a D″ layer with traverse isotropy such as could be produced by hexagonally symmetric crystals with the symmetry axis orientated vertically or by stacks of horizontal thin layers with strong velocity contrasts[23–25]. The anisotropic zone must extend up at least several hundred kilometres above the CMB.

Under the central Pacific there are rapid spatial variations in shear-wave splitting, sometimes with SH arriving ahead of SV, sometimes with SV arriving ahead of SH, and sometimes with shear-wave splitting that is not aligned with the great-circle reference frame[26,42–44] (Fig. 2b). Although azimuthal coverage is again limited, the observations are consistent with patchy regions of general (triclinic) anisotropy or hexagonal symmetry with either vertical or horizontal symmetry axes. Many paths with no evidence for shear-wave splitting are also found. When observed, the anisotropy beneath the Pacific appears to be confined to the lowermost portion of D″, as it tends to increase with distance and, hence, turning-point depth of the seismic rays (Fig. 1a). It is hard to resolve the radial scale of the anisotropic zone owing to strong trade-offs with its lateral extent and ray-path sensitivity to lateral heterogeneity, but the observed rapid fluctuations suggest a thickness of less than 100 km. Although interpretation of deep-mantle shear-wave anisotropy is fraught with uncertainty, as discussed below, it appears that there must be a fundamental difference in structure, deformation style and/or chemistry between the D″ region and the overlying mantle.

## D″ discontinuity

Over the past 15 years, there has been extensive mapping of the D″ P- and S-wave discontinuities involving more than 40 different studies[21], with the shear-wave structure being extensively detected as shown in Fig. 2c. Many areas have not been analysed owing to the limitations of the source/receiver distribution for analysing reflections from the discontinuity. Where detected, the discontinuity has been successfully modelled as having a strength of 1.5–3% and a depth of 250 ± 100 km above the CMB. The structure appears to be more variable for P waves than for longer-period S waves, and in some places the 'discontinuity' may in fact be a gradational transition zone of up to 50 km thickness rather than an abrupt contrast. In localized patches the discontinuity has either 100–300 km wavelength topography of about 50 km height or corresponding acute lateral gradients in velocity structure, based on the fluctuations in amplitudes and travel times of the reflected phases[45,46]. The small-scale variability raises the possibility that the discontinuity represents a transition between mantle regions with contrasting physical properties, such as anisotropic fabric or extent of chemical heterogeneity, rather than a conventional rock boundary.

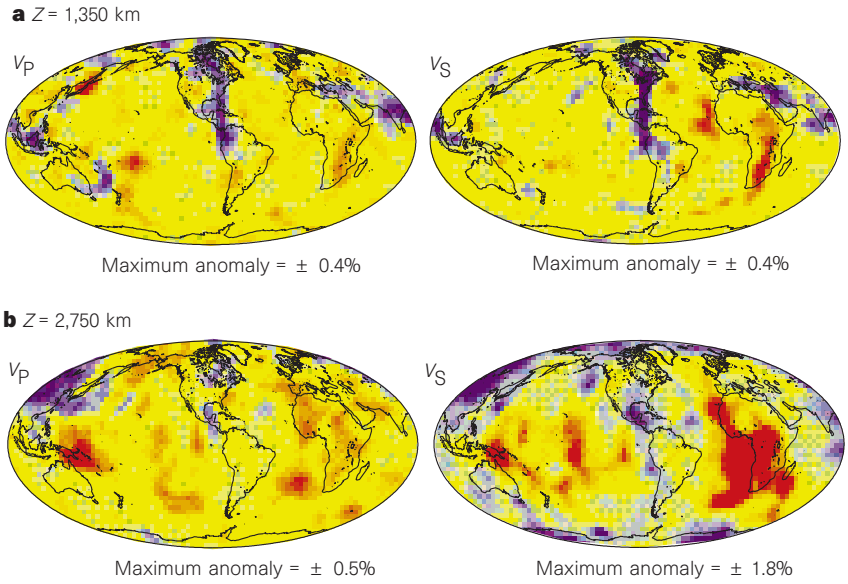


**Figure 3** Recent high-resolution global seismic tomography models for P-wave[31] and S-wave[30] velocity heterogeneity near depths (*Z*) of 1,350 km (top row) and 2,750 km (bottom row). Faster than average velocities are indicated by blues, and slower than average velocities are indicated by reds, with the peak velocity anomaly being shown for each panel (P-wave velocity, $V_P$ left column; S-wave velocity, $V_S$, right column). We note the much larger amplitudes of the shear-wave velocity heterogeneity in the D″ layer. The mid-mantle structure appears to be dominated by tabular high-velocity structures, which are generally interpreted to be deep downwellings, possibly associated with slabs penetrating into the lower mantle. These features tend to have coherent over large depth ranges. The D″ layer is dominated by large-scale heterogeneities that have limited spatial systematics related to mid-mantle features.

The velocity gradient within the D″ layer beneath the velocity discontinuity appears to be slightly negative, extending over most of the 200–300 km layer thickness[21]. The shear-wave velocity discontinuity is detected by both SH and SV waves, but appears to have weaker strength for SV in the area below Alaska[47], suggesting that the discontinuity is itself associated with the seismic anisotropy observed in this region[24,25]. Similarly, there is good evidence for the presence of a shear velocity discontinuity beneath the Caribbean, in the vicinity of the region showing coherent transverse isotropy[20,23,48].

## Spatial correlations in D″ characteristics

Given the limited spatial coverage of the unusual seismic features in D″ apparent in Fig. 2, establishing any association between these detailed features and the relatively large-scale variations detected throughout the mantle by travel-time tomography can allow global interferences to be made. Heterogeneity patterns of P- and S-wave velocities from recent high-resolution tomographic inversions[30,31] are shown for the mid-mantle depth of 1,350 km and the mid-D″ depth of 2,750 km in Fig. 3. Of particular interest are possible relations between mid-mantle structures that appear to be dominated by slab-like fast velocity (if these are thermal anomalies, they will be colder, denser, and hence downwelling) heterogeneities (possibly oceanic slabs) and D″ structures. A significant transition in the lateral scale length of heterogeneities between the mid-mantle and the D″ region is apparent in Fig. 3, even allowing for incomplete spatial sampling, and the strength of shear-wave velocity heterogeneity appears to be particular acute in the D″ region[31].

The region beneath the central Pacific with the extensive ULVZ in Fig. 2a corresponds to a large-scale low-velocity feature in the tomography models, but there is not a universal correlation between

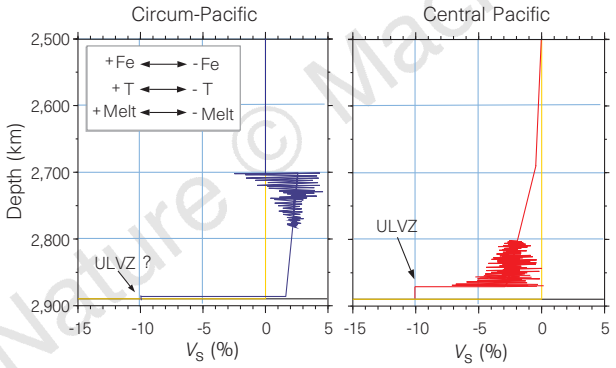


**Figure 4** The main classes of D″ shear-wave velocity structures. Schematic shear-wave velocity structures (shown as per cent deviations ($\delta V_S$) relative to a standard reference Earth model which has smoothly varying structure in the lower mantle) for circum-Pacific (left) and central Pacific (right) regions. The circum-Pacific regions under Alaska and the Caribbean are well characterized to have relatively abrupt shear velocity increases near 250 km above the CMB, with mild negative gradients throughout the D″ layer. The blue model indicates that these high-velocity regions are relatively cold. These regions also have shear-wave splitting consistent with transverse isotropy, which is represented here by thin horizontal lamellae of strongly varying material properties (possibly involving melt), concentrated near the depth of the discontinuity. Any ULVZ in these regions is so thin as to not be detectable in most cases, and it may not be present. The central Pacific region is characterized by strong negative gradients of shear velocity extending over 200–300 km above the CMB, with little evidence for any discontinuity. The red model indicates that these low-velocity regions are relatively hot. This region has a thick, pronounced ULVZ, with shear velocity decreases that are of the order of 5–30%. There appears to be laterally variable general anisotropy, concentrated towards the base of the D″ region (and possibly in the ULVZ as well). The sense of velocity perturbation with respect to increasing or decreasing Fe concentration, temperature (*T*) or partial melt is indicated by the inset box.

ULVZ presence and slow D″ structure. The central-Pacific low-velocity region is a relatively stable feature among different tomographic models, and detailed localized studies indicate that the shear-wave velocity has a strongly negative gradient in the lowermost 200–300 km in this general region, with only intermittent evidence for a shear-wave velocity discontinuity[49]. This zone of negative gradient, like the zones of weaker negative gradient beneath regions that have a shear-wave velocity discontinuity, is significantly thicker than the 50–75 km thickness that is often proposed for a thermal boundary layer above the CMB[50].

The spatial relationship between locations with an observed shear-wave velocity discontinuity and large-scale fast or slow velocity structure in D″ is complex. There is a general tendency for circum-Pacific regions to have higher than average velocities in the data shown in Fig. 3 as well as in lower-resolution tomographic models[10–12], but the overall correlation with either P- or S-wave velocity discontinuities is weak[21]. Similarly, any relationship between high-velocity mid-mantle features and the presence of D″ discontinuities is weak: this is perhaps not surprising given that the scale length of lateral heterogeneities appears to shift with depth (Fig. 3).

It is premature to formulate any simplified characterization of how the seismic observations are interrelated on a global basis. Nonetheless, for several of the best-studied regions, there are clear associations that may be summarized as the characteristic dichotomous shear-wave velocity structures in Fig. 4. Regions like those beneath Alaska and the Caribbean have relatively high shear-wave velocities in D″, with a 2–3% SH velocity increase near 200–280 km above the CMB. This velocity increase appears to be weaker for SV, which is consistent with the presence of transverse isotropy that can explain early SH arrivals. This is represented in Fig. 4 by strongly fluctuating horizontal lamellae with high-velocity-contrast materials. Such a laminated structure can account for long-wavelength transverse isotropy[51], but alternative possibilities are discussed below. The velocity gradient throughout the D″ region appears to be negative in these areas, and the strength of lateral heterogeneity reduces with depth. Any ULVZ in these areas is either very intermittent or so thin as to be nondetectable.

In contrast, an area like the central Pacific is characterized by a structure with no significant discontinuity, a strong negative velocity gradient over a depth range of 200 km or more, a thick (up to 40 km) ULVZ, and laterally variable anisotropic structure that appears to be concentrated towards the deeper portion of D″. The central-Pacific anisotropy appears to involve general anisotropy possibly with, in some cases, horizontal symmetry axes such as would be associated with vertical laminations. Although the structures in D″ are undoubtedly not strictly dichotomous, there appear to be large coherent regions with the basic features shown in Fig. 4. These seismological features, and their spatial extent, constitute primary new observational constraints on the thermochemical processes in the lowermost mantle that require interpretations based on our understanding of the physical properties and dynamics of materials at extreme pressures and temperatures. Notably, ideas associated with a simple subsolidus thermal boundary layer are unable to account for most of the features in Fig. 4.

## Thermochemical implications

Our knowledge of the complexity of the lowermost mantle has burgeoned over the past 15 years from a zone of decreased compressional- and shear-wave velocity gradients relative to the overlying lower mantle to a zone with pervasive multi-scale heterogeneity, laterally varying seismic discontinuities at depths about 250 km above (and also just above) the CMB, and the presence of variable seismic anisotropy. This challenges computational, theoretical and experimental geophysics to produce viable models for the structure, temperature, flow pattern and chemistry of the lowermost mantle. There has been extensive consideration of possible

connections between the CMB and surface observables, with plume-like upwellings rising from a hot CMB thermal boundary layer to generate hotspot volcanism at the surface, and subduction-related cold downwellings producing locally seismically fast (and geochemically anomalous) zones at the CMB. Yet, recent developments in seismology, experimental geophysics and geodynamics indicate that the interaction between hot upwellings, cold downwellings and the CMB are more complex than previously recognized: partial melting, core–mantle chemical interactions, and resultant chemical heterogeneities may each play a role in the dynamic coupling of this layer with the overlying pattern of mantle convection and surface tectonics.

## Plumes and the lowermost mantle

The idea that the CMB gives rise to plume-like instabilities and volcanic centres called hotspots is firmly rooted in fluid dynamic experiments and calculations[5–7,52–55]. Such upwellings require a boundary layer heated from below, and a lowered viscosity within both the plume and a basal layer which serves as a feeder zone for the plume[52,53,55]. Fluid dynamic stability analysis indicates that the distribution of surface hotspots places a bound of $\geqslant 10^6$ on the viscosity contrast between such a basal boundary layer and the overlying mantle[54]. As viscosity of minerals is strongly temperature dependent[56], this lower bound on the boundary layer viscosity contrast could be generated by a temperature jump of 1,000 K, in accord with estimates of the temperature increase across D″[3,4]. Larger changes in viscosity could be generated by the presence of partial melting at the base of the mantle[29,35,36]: the spatial correlation of the ULVZ with hotspots (Fig. 5 and ref. 57) indicates that deep-seated partial melt may enhance the ascent of a plume to the surface.

Both petrological modelling of upper-mantle plumes and seismic modelling of lower-mantle variations predict plume excess-temperature anomalies of only about 300 K (refs 58, 59), far less than inferred for plumes ascending from a boundary layer with a temperature increase near 1,000 K (refs 3, 4). Neither entrainment of surrounding material into the ascending plume[60], nor diffusional loss of heat from the plume[61], explain this discrepancy. However, imposing a chemical boundary layer at the base of D″ which is denser by at least 5–10% than the overlying mantle decreases the excess temperature of plumes to values in accord with observations[62]. In effect, a chemically stratified boundary layer produces plume extraction from mid-way within the basal thermal boundary layer. Yet the nature of such a chemical boundary layer remains unclear, as do the geodynamic implications of profoundly depressed viscosities in a layer at the base of the mantle. To date, numerical convection simulations have typically not incorporated basal viscosity contrasts which approach a factor of $10^6$ or greater: the coupling of large viscosity contrasts with a chemically zoned, laterally heterogeneous boundary layer represents the next generation of geodynamic calculations on CMB properties.

The prevailing view of hotspot generation may thus evolve from one in which plumes originate at the bottom of a thermal boundary layer in a chemically homogeneous mantle, to one in which plumes emerge from a depth some tens of kilometres above the CMB—either within the upper portions of, or above a chemically distinct, partially molten zone (Fig. 6). The zone from which plumes extract material is likely to be both highly inviscid and chemically different from the overlying mantle. The degree and manner in which plumes derived in this way would record a geochemical signature of interaction with the Earth's core are unclear, although hints of such a signature have been reported[63].

As plumes have been proposed to have a causal relationship with continental extension and breakup at the surface of the Earth[53,64], there is considerable importance in understanding not only the detailed thermochemical dynamics which give rise to plumes, but also the likely evolution of plumes over Earth's history, from the perspective of CMB processes. For example, if the basal portion of D″ has been progressively enriched in relatively dense components over time, a decrease in the excess temperature of such D″-derived upwellings would have expected over Earth's history: in this sense, the detailed (and obscure[65]) history of hotspot volcanism may provide the only constraints on the properties of the past CMB.

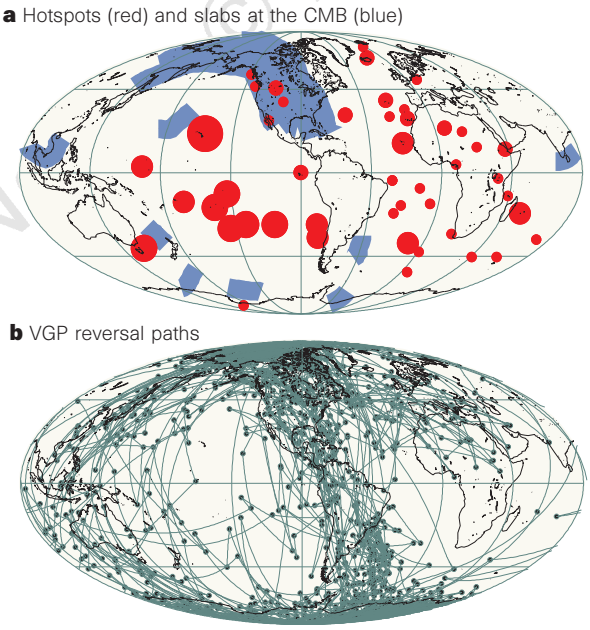


**Figure 5** Spatial patterns of large-scale mantle and core dynamical structures. **a**, Map showing spatial distribution of subducted slabs that are expected to have penetrated to the base of the mantle[94] (blue lines) and buoyancy flux weighted hotspots[6,54] (red dots). **b**, Map showing virtual geomagnetic pole (VGP) reversal paths[83] (green lines). To first order, reversal paths and hotspots appear to be anti-correlated, with reversal paths generally following approximately longitudinal bands in which the ULVZ has not been observed to be present (Fig. 2).

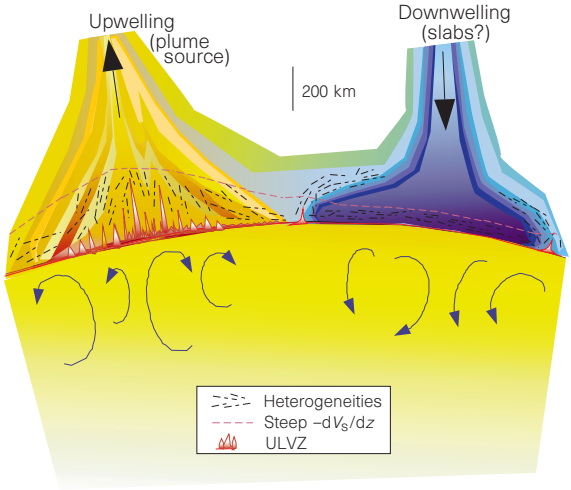


**Figure 6** Diagram of possible large-scale CMB structures. The chemical heterogeneities schematically illustrated may arise from partial melting, core–mantle reaction products, slab-associated geochemical heterogeneities, or a combination of these effects. The shape of downwellings at the CMB and the manner in which they interact with CMB structure is unclear (Fig. 3). In the scheme drawn here, the negative buoyancy associated with the downwelling is sufficient to displace much of the pre-existing CMB structure.

## Core–mantle chemical reactions

Dynamical simulations indicate that maintaining compositional heterogeneities within D″ requires density increases greater than about 6% to avoid entrainment into the overlying convecting mantle over time[66,67]. The mechanisms by which such dense material could be introduced into D″ involve either interactions with the underlying core or descent of denser material from the overlying mantle. Chemical reactions between iron alloys and silicates have been shown to occur at high pressures from both experimental and thermodynamic perspectives[16,68–70]: such reactions are of the form

$$(Mg_xFe_{1-x})SiO_3 + 3[1-x) - s]Fe = xMgSiO_3 + sSiO_2 + [(1-x) - s]FeSi + [3(1-x) - 2s]FeO$$

where $1 - x$ is the amount of iron in reacting mantle material, and $s$ is the amount of silica generated by the reaction[16]. This reaction of iron with mantle material is uniquely a high-pressure phenomenon, as it does not occur at pressures below about 20–30 GPa (refs 16, 68). The unusual feature of this reaction is that its products—silicates and iron alloys—differ profoundly in their densities and likely thermal and electrical conductivities.

If pervasive core–mantle chemical reactions occur at the CMB, and if FeSi and FeO are able to segregate from their complementary $MgSiO_3$ and $SiO_2$, a dense, highly conductive iron-alloy layer could be generated[71]. Although the extent of reactions of core material with the mantle remains controversial[17], it is notable that such reactions are markedly enhanced if the reacting silicates are molten[70]. Accordingly, one possible explanation for the manner in which a chemically distinct (and possibly chemically stratified), partially molten layer at the base of the mantle could arise involves varying amounts of reaction between a partially molten layer at the base of the mantle and the outer core, with increasing degrees of reaction as a function of depth. The flow regime within a partially molten basal layer remains obscure[26], but any upward flow within such a layer would produce non-diffusion-limited transfer of iron from the outer core into the lowermost mantle[16,17], while simultaneously tending to reduce the amount of stratification within the layer.

## Chemical heterogeneities from the mantle

Segregation of dense material from the overlying mantle into D″ could occur by downward descent of negatively buoyant liquids or solids.We speculate that partial melt in the lower mantle could be denser than its coexisting solids[72], particularly if iron partitions preferentially into the liquid, as it does at lower pressures[73,74]. Indeed, the relatively high ratio of S-wave velocity changes to P-wave velocity changes in the bulk of the lower mantle has been attributed to small degrees of partial melting[75]. If the ULVZ is produced by downward descent of melt from the overlying mantle, then it would be anticipated to be enriched in incompatible (and possibly volatile) elements[76], and would differ in its composition from mantle that was altered through interaction with the core and melted *in situ* at the CMB. Unfortunately, the properties of melts under deep mantle conditions are largely uncontrained by experiment: both the temperature and composition of the solidus of the lower mantle are unknown at CMB conditions. Therefore, the probable chemistry of the ULVZ remains almost completely conjectural, other than the single observation that material of $(Mg, Fe)_2SiO_4$ composition appears to undergo eutectic-style melting at CMB pressures and temperatures near 4,300 K (ref. 77). From an experimental viewpoint, the melting behaviour of the lowermost mantle remains a largely unaccessed frontier: both the eutectic chemistry and temperature of likely lower mantle assemblages are ill-constrained, as are the effects of volatile- and iron-enrichment of such material.

Descent of solid material into D″ from the overlying mantle could also alter the chemistry of the lowermost mantle. This may involve subduction-related processes: chemically differentiated oceanic crustal material might penetrate to D″ providing a distinctive hotspot geochemical reservoir[8,9], and possibly generating laminated features that cause seismic anisotropy of the lowermost mantle[23]. Although the presence in D″ of material derived from oceanic lithosphere cannot be precluded, the persistence of tabular downwellings to the base of the mantle is suggested in only a few regions[30,31]. As cold thermal anomalies, slab-related downwellings have long been recognized to be anticorrelated with hotspots[78] (Fig. 5). Such downwellings, if they impinge on D″, may produce a generally different structure at the base of the mantle than is present in zones of upwellings, and it is this dichotomy which may give rise to the end-member velocity profiles of Fig. 4.

## Mechanisms for generating anisotropy in D″

Both downwellings and upwellings should give rise to strong shear flows near the CMB (Fig. 6) that may produce anisotropy in D″. Yet, the very observation of anisotropy in this zone is anomalous relative to the isotropic character of the overlying lower mantle which presumably also has strong shear flows[41]. The two primary means for producing D″ anisotropy are through the presence of structural laminations of material with a shear modulus which differs from that of the surrounding mantle, or a shift in the deformation mechanisms producing flow within the boundary layer. Possibilities for producing structural laminations in this region include emplacement of subducted oceanic crust (possibly partially molten), core–mantle reaction products swept up by mantle flow, or orientated inclusions of partial melt[23,26]. Indeed, orientated melt inclusions are particularly efficient at generating the observed anisotropy of the lowermost mantle[23]. If partial melt is ubiquitous and variable in its depth extent in the lowermost mantle[35,36], and if strain fields near upwellings and downwellings are sufficiently strong, a lateral smearing of locally elevated partially molten regions could result from the combination of melt and lateral flow at these depths. Such a process is schematically illustrated in Fig. 6, in which the heterogeneous straining of the upper portion of a partially molten zone could generate layered (and anisotropic) structure such as are shown in Fig. 4.

Alternatively, anisotropy might be generated if either the strain history of the lowermost mantle dramatically differs from that of the overlying material,or if there is a shift in ability to acquire anisotropic fabric within the thermal boundary layer at the base of the mantle. Such a shift could be induced by either a change in mineral phase or a change in the deformation regime of the lowermost mantle. There is little evidence for any phase change occurring in any significant lower-mantle mineralogical constituent in the lowermost 300 km of the mantle[26]. It is possible that the increased temperatures within D″ could drive the deformation mechanism of the deep mantle from a superplastic regime[79] into a regime of power-law creep. Deformation maps for a range of materials (including olivine) indicate that increasing temperature at moderately high (and constant) shear stress induces such a transition from superplastic flow to power-law creep[80]. The former deformational mechanism is expected to produce notably less preferred orientation than the latter: such a shift in deformational mechanism could produce an apparent onset of anisotropy within D″. Although the virtually unconstrained depth-dependence of shear stress in the lowermost mantle could also play a primary role in modulating the deformational regime and the resultant magnitude of preferred orientation, the existence of anisotropy within D″ could be simply a manifestation of either the hotter temperature in this region or of the flow regime producing stretching of melt inclusions. In either case, the presence of anisotropy is expected to reflect the direction of the local flow and, as such, observations of anisotropy have the prospect of providing a fundamental signature of the direction, depth extent, and lateral variability of the geodynamic flow pattern in the basal boundary layer of Earth's mantle.

## Mechanisms for producing D″ discontinuities

The physical and/or chemical changes that produce laterally sporadic discontinuities near 250 km (refs 21, 34) above the CMB remain obscure. The lateral variations in discontinuities (Fig. 2) probably precludes their explanation by a pressure-induced phase transition of a significant lower-mantle constituent, particularly given the lack of observation of such transitions in the main lower-mantle minerals at these pressures[21,26]. High-pressure transitions in $SiO_2$ have been proposed to play a role in D″ structure[81], but the manner in which large (and laterally variable) quantities of free silica could be produced in the lowermost mantle is not clear. The possibility that subducted slabs, which are chemically stratified and may maintain a thermally cold signature to depths of the CMB, could produce these discontinuities presents a few difficult, although perhaps not insurmountable, dynamic issues[21]. These include how the thermally cold core (or perhaps basaltic top) of subducted slabs with initial thickness of near 150 km might become essentially horizontally emplaced at depths near 250 km above the CMB. Such a vertically and laterally homogeneous emplacement implies a coherent deposition of the slab above the CMB that is not apparent in the present images of downwellings in this region (Fig. 3). The possible correlation of these discontinuities with observations of D″ anisotropy (Fig. 2) indicates that their shear velocity contrast could be partially associated with the onset of pervasive texturing or preferred alignment of minerals within D″. That the precise cause(s) of the discontinuity 250 km above the CMB remains enigmatic illustrates the broad range of uncertainties which accompany present geodynamic and mineralogic inferences about the basal structure of the mantle: high-pressure experiments on mantle assemblages at CMB pressures remain in their infancy, and material properties required for accurate geodynamic simulations (such as the magnitude of local density and viscosity contrasts) are poorly constrained.

## Magnetic-field implications

Compositional variations and partial melting above the CMB have potentially profound implications both for propagation of the geomagnetic field through the mantle and for the manner in which the magnetic field reverses. The magnetic field is produced by fluid flow within the molten metallic outer core, but a heterogeneous high-conductivity layer within the mantle would be expected to produce a screening effect on the core-generated field and a resultant electromagnetic torque on the deep mantle: such a torque may produce observed decadal fluctuations in the Earth's rotation rate[82]. Moreover, the amount of heat flow into the base of the mantle from the core (and thus the flow pattern at the top of the outer core) is controlled by the temperature field within the lowermost mantle: this temperature distribution could be altered by shifts in plume flux. Indeed, a coupling between plume activity, the temperature field in the lowermost mantle, and the frequency of reversals of the geomagnetic field has been proposed to exist[83,84].

Qualitatively, there appears to be an anti-correlation between the paths taken by the Earth's pole during magnetic field reversals[85] and distribution of the ULVZ (Figs 2 and 5). Although the existence of preferred reversal paths is controversial[86,87], it is possible that the lowermost mantle influences the manner in which the magnetic field reverses, or may control the surface manifestation of reversals[84]. But the detailed cause of any coupling between the deep mantle and the magnetic field remains uncertain: correlations between reversal paths and deep mantle structure may be generated with the present field strength if the electrical conductivity of the lowermost mantle lies within two orders of magnitude of that of the core[88]. Short-period shifts ("jerks") in the field intensity may indicate, however, that low-conductivity regions exist near the CMB as well[89]. Iron enrichment of the lowermost boundary could certainly enhance the electrical conductivity of the mantle side of the CMB[16,70,90]. Few data exist on the electrical conductivity of melted or partially molten lower-mantle assemblages, but those which do exist are consistent with an increased conductivity of molten silicates of between one and two orders of magnitude relative to solid silicates[91]. Therefore, an iron-enriched, partially molten zone at the base of the mantle could potentially access electrical conductivities which could influence the manner in which reversals of the geomagnetic field occur, as well as alter the present observed field at the surface of the Earth. Indeed, if the ULVZ is associated with high electrical conductivities, than its lateral variability (Fig. 2) may produce a partially shuttered window through which we view the Earth's magnetic field.

## The CMB and deep mantle dynamics

The recognition of laterally heterogeneous layering and likely signatures of vertical and lateral flow near the CMB has dramatically enhanced the complexity of processes attributed to the region. The presence of the largest seismic discontinuity within Earth's mantle at a scant 5–40 km above the CMB, and its association with the onset of partial melting at this depth, has profound implications not only for deep mantle structure, but also potentially for the genesis of hotspots (and thus possibly continental extension at the Earth's surface, as well) and for the properties of the geomagnetic field. The demonstration that the D″ region is the only portion of the lowermost 2,100 km of the Earth's mantle that shows evidence for anisotropy, implying texturing by flow of material at these depths, indicates that it may actually be possible to characterize flow patterns in this dynamic boundary layer.

In spite of these advances, important questions remain. Despite its discovery nearly 15 years ago, the physical origin of the seismic discontinuity lying near 250 km above the CMB remains enigmatic. The manner in which cold downwellings interact with the basal layer of the mantle is unclear, as is the complementary issue of whether slab-associated material ultimately becomes incorporated within the D″ region. In both the amount (and nature) of chemical input derived from downwellings from above, and in the degree to which interaction of D″ with the underlying core occurs, the chemistry of the bottom of the mantle (and particularly of any partially molten zones) continues to be uncertain. As the probable source region for plumes, the temporal evolution of structure at the CMB may be of crucial importance for understanding the geochemical and thermal evolution of our planet. Indeed, it is not known whether the ULVZ has been gradually produced over time by a combination of core interactions and iron- and/or volatile-enriched melts descending from above, or whether it represents the last residue of a terrestrial magma ocean[92], pinned by negative buoyancy at the base of a thermal boundary layer.

The rapidity with which new structures within D″ have been seismically characterized has (for the moment) outpaced the corresponding interpretive geodynamic and experimental work. Indeed, few studies have been conducted to date which were designed to constrain the nature of the newly discovered seismic structures of this region. Because of the importance of this region, and because of the temporary offset between the observations and interpretive studies—coupled with the accelerating number and enhanced quality of seismic observations—it seems likely that the CMB is about to replace the transition zone between Earth's upper and lower mantle as the region most likely to hold the key to a large number of geophysical problems[93]. □

*T. Lay and Q. Williams are in the Earth Sciences Department, University of California, Santa Cruz, California 95064, USA; E. J. Garnero is in the Seismological Laboratory, University of California, Berkeley, California 94720, USA.*

1. Lay, T. Structure of the core-mantle transition zone: A chemical and thermal boundary layer. *Eos* **70,** 54–55, 58–59 (1989).
2. Loper, D. E. & Lay, T. The core-mantle boundary region. *J. Geophys. Res.* **100,** 6397–6420 (1995).
3. Williams, Q. & Jeanloz, R. Melting relations in the iron-sulfur system at high pressures: Implications for the thermal state of the Earth. *J. Geophys. Res.* **95,** 19299–19310 (1990).
4. Boehler, R. Temperatures in the Earth's core from melting-point measurements of iron at high static pressures. *Nature* **363,** 534–536 (1993).

5. Davies, G. F. Ocean bathymetry and mantle convection, 1, Large-scale flow and hotspots. *J. Geophys. Res.* **93,** 10447–10480 (1988).
6. Sleep, N. H. Hotspots and mantle plumes: Some phenomenology. *J. Geophys. Res.* **95,** 6715–6736 (1990).
7. Loper, D. E. Mantle plumes. *Tectonophysics* **187,** 373–384 (1991).
8. Hoffman, A. W. & White, W. M. Mantle plumes from ancient oceanic crust. *Earth Planet. Sci. Lett.* **57,** 421–436 (1982).
9. Woodhead, J. D., Greenwood, P., Harmon, R. S. & Stoffers, P. Oxygen isotope evidence for recycled crust in the source of EM-type ocean island basalts. *Nature* **362,** 809–813 (1993).
10. Su, W-J., Woodward, R. & Dziewonski, A. M. Degree 12 model of shear velocity heterogeneity in the mantle. *J. Geophys. Res.* **99,** 6945–6980 (1994).
11. Li, X. D. & Romanowicz, B. Global mantle shear velocity model developed using nonlinear asymptotic coupling theory. *J. Geophys. Res.* **101,** 22245–22272 (1996).
12. Masters, T. G., Johnson, S., Laske, G. & Bolton, H. A shear-velocity model of the mantle. *Phil. Trans. R. Soc. Lond. A* **354,** 1385–1411 (1996).
13. Gubbins, D. Core-mantle interactions. *Tectonophysics* **187,** 385–391 (1991).
14. Bloxham, J. & Jackson, A. Fluid flow near the surface of Earth's outer core. *Rev. Geophys.* **29,** 97–120 (1991).
15. Hide, R., Speith, M. A., Clayton, R. W., Hager, B. H. & Voorhies, C. V. in *Relating Geophysical Structures and Processes: The Jeffreys Volume* (eds Aki, K. & Dmowska, R.) 107–120 (Geophys. Monogr. Ser. 76, Am. Geophys Union, Washington DC, 1993).
16. Knittle, E. & Jeanloz, R. Earth's core-mantle boundary: Results of experiments at high pressures and temperatures. *Science* **251,** 1438–1443 (1991).
17. Poirier, J.-P. Core-infiltrated mantle and the nature of the D″ layer. *J. Geomagn. Geoelectr.* **45,** 1221–1227 (1993).
18. Lay, T. Seismology of the lower mantle and core-mantle boundary. *Rev. Geophys. Suppl.* 325–328 (1995).
19. Weber, M. *et al.* in *Seismic Modeling of the Earth's Structure* (eds Boschi, E., Ekström, G. & Morelli, A.) 399–442 (Istit. Naz. di Geophys., Rome, 1996).
20. Ding, X. & Helmberger, D. V. Modeling D″ structure beneath Central America with broadband seismic data. *Phys. Earth Planet Inter.* **101,** 245–270 (1997).
21. Wysession, M. E. *et al.* The D″ discontinuity and its implications. in *The Core-Mantle Boundary* (eds Gurnis, M., Buffett, B. A., Knittle, E. & Wysession, M.) (Am. Geophys. Union, in the press).
22. Vinnik, L., Romanowicz, B., Le Stunff, Y. & Makeyeva, L. Seismic anisotropy in the D″ layer. *Geophys. Res. Lett.* **22,** 1657–1660 (1995).
23. Kendall, J.-M. & Silver, P. G. Constraints from seismic anisotropy on the nature of the lowermost mantle. *Nature* **381,** 409–412 (1996).
24. Matzel, E., Sen, M. K. & Grand, S. P. Evidence for anisotropy in the deep mantle beneath Alaska. *Geophys. Res. Lett.* **23,** 2417–2420 (1996).
25. Garnero, E. J. & Lay, T. Lateral variations in lowermost mantle shear wave anisotropy beneath the north Pacific and Alaska. *J. Geophys. Res.* **102,** 8121–8135 (1997).
26. Lay, T., Garnero, E. J., Williams, Q., Kellogg, L. & Wysession, M. E. Seismic wave anisotropy in the D″ region and its implications. in *The Core-Mantle Boundary* (eds Gurnis, M., Buffett, B. A., Knittle, E. & Wysession, M.) (Am. Geophys. Union, in the press).
27. Garnero, E. J. & Helmberger, D. V. A very slow basal layer underlying large-scale low-velocity anomalies in the lower mantle beneath the Pacific: evidence from core phases. *Phys. Earth Planet. Inter.* **91,** 161–176 (1995).
28. Mori, J. & Helmberger, D. V. Localized boundary layer below the mid-Pacific velocity anomaly identified from a PcP precursor. *J. Geophys. Res.* **100,** 20359–20365 (1995).
29. Garnero, E. J., Revenaugh, J., Williams, Q., Lay, T. & Kellogg, L. Ultra-low velocity zone at the core-mantle boundary. in *The Core-Mantle Boundary* (eds Gurnis, M., Buffett, B. A., Knittle, E. & Wysession, M.) (Am Geophys. Union, in the press).
30. Grand, S. P., van der Hilst, R. D. & Widiyantoro, S. Global seismic tomography: A snapshot of convection in the Earth. *GSA Today* **7,** 1–7 (1997).
31. van der Hilst, R. D., Widiyantoro, S. & Engdahl, E. R. Evidence for deep mantle circulation from global tomography. *Nature* **386,** 578–584 (1997).
32. Young, C. J. & Lay, T. The core mantle boundary. *Annu. Rev. Earth Planet. Sci.* **15,** 25–46 (1987).
33. Wysession, M. E. Large scale structure at the core-mantle boundary from core-diffracted waves. *Nature* **382,** 244–248 (1996).
34. Lay, T. & Helmberger, D. V. A lower mantle *S*-wave triplication and the shear velocity structure of D″. *Geophys. J. R. Astron. Soc.* **75,** 799–838 (1983).
35. Williams, Q. & Garnero, E. J. Seismic evidence for partial melt at the base of Earth's mantle. *Science* **273,** 1528–1530 (1996).
36. Revenaugh, J. S. & Meyer, R. Seismic evidence of partial melt within a possibly ubiquitous low velocity layer at the base of the mantle. *Science* **277,** 670–673 (1997).
37. Garnero, E. J. & Helmberger, D. V. Seismic detection of a thin laterally varying boundary layer at the base of the mantle beneath the central-Pacific. *Geophys. Res. Lett.* **23,** 977–980 (1996).
38. Bataille, K., Wu, R. S. & Flatté, S. M. Inhomogeneities near the core-mantle boundary evidenced from scattered waves: A review. *Pure Appl. Geophys.* **132,** 151–174 (1990).
39. Vidale, J. E. & Hedlin, M. A. H. Evidence for partial melt at the core–mantle boundary north of Tonga from the strong scattering of seismic waves. *Nature* **391,** 682–685 (1998).
40. Kaneshima, S. & Silver, P. G. A search for source-side anisotropy. *Geophys. Res. Lett.* **19,** 1049–1052 (1992).
41. Meade, C., Silver, P. G. & Kaneshima, S. Laboratory and seismological observations of lower mantle isotropy. *Geophys. Res. Lett.* **22,** 1293–1296 (1995).
42. Pulliam, J. & Sen, M. K. Seismic anisotropy in the core-mantle transition zone. *Geophys. J. Int.* (in the press).
43. Kendall, J.-M. & Silver, P. G. Investigating causes of D″ anisotropy. in *The Core-Mantle Boundary* (eds Gurnis, M., Buffett, B. A., Knittle, E. & Wysession, M.) (Am Geophys. Union, in the press).
44. Ritsema, J., Lay, T., Garnero, E. J. & Benz, H. Seismic anisotropy in the lowermost mantle beneath the Pacific. *Geophys. Res. Lett.* (in the press).
45. Weber, M. P and S wave reflections from anomalies in the lowermost mantle. *Geophys. J. Int.* **115,** 183–210 (1993).
46. Lay, T., Garnero, E. J., Young, C. J. & Gaherty, J. B. Scale-lengths of shear velocity heterogeneity at the base of the mantle from S wave differential travel times. *J. Geophys. Res.* **102,** 9887–9910 (1997).
47. Lay, T. & Young, C. J. Analysis of seismic SV waves in the core's penumbra. *Geophys. Res. Lett.* **18,** 1373–1376 (1991).
48. Kendall, J.-M. & Nangini, C. Lateral variations in D″ below the Caribbean. *Geophys. Res. Lett.* **23,** 399–402 (1996).
49. Ritsema, J., Garnero, E. & Lay, T. A strongly negative shear velocity gradient and lateral variability in the lowermost mantle beneath the Pacific. *J. Geophys. Res.* **102,** 20395–20411 (1997).
50. Stacey, F. D. & Loper, D. E. The thermal boundary layer interpretation of D″ and its role as a plume source. *Phys. Earth Planet. Inter.* **33,** 45–55 (1983).
51. Backus, G. E. Long-wave elastic anisotropy produced by horizontal layering. *J. Geophys. Res.* **67,** 4427–4440 (1962).
52. Whitehead, J. A. & Luther, D. S. Dynamics of laboratory diapir and plume models. *J. Geophys. Res.* **80,** 705–717 (1975).
53. Duncan, R. A. & Richards, M. A. Hotspots, mantle plumes, flood basalts, and true polar wander. *Rev. Geophys.* **29,** 31–50 (1991).
54. Ribe, N. M. & de Valpine, D. P. The global hotspot distribution and instability of D″. *Geophys. Res. Lett.* **21,** 1507–1510 (1994).
55. Bercovici, D. & Kelly, A. The non-linear initiation of diapirs and plume heads. *Phys. Earth Planet. Inter.* **101,** 119–130 (1997).
56. Karato, S. & Li, P. Diffusion creep in perovskite: Implications for the rheology of the lower mantle. *Science* **255,** 1238–1240 (1992).
57. Williams, Q., Revenaugh, J. & Ganero, E. J. A correlation between ultralow basal velocities in the mantle and hotspots. *Science* (submitted).
58. Watson, S. & McKenzie, D. P. Melt generation by plumes: A study of Hawaiian volcanism. *J. Petrol.* **12,** 501–537 (1991).
59. Nataf, H.-C. & vanDecar, J. Seismological detection of a mantle plume? *Nature* **264,** 115–120 (1993).
60. Farnetani, C. G. & Richards, M. A. Thermal entrainment and melting in mantle plumes. *Earth Planet. Sci. Lett.* **136,** 251–267 (1995).
61. Leitch, A. M., Steinbach, V. & Yuen, D. A. Centerline temperature of mantle plumes in various geometries: Incompressible flow. *J. Geophys. Res.* **101,** 21928–21846 (1996).
62. Farnetani, C. G. Excess temperature of mantle plumes: The role of chemical stratification across D″. *Geophys. Res. Lett.* **24,** 1583–1586 (1997).
63. Walker, R. J., Morgan, J. W. & Horan, M. F. Osmium-187 enrichment in some plumes—evidence for core-mantle interaction. *Science* **269,** 819–822 (1995).
64. Storey, B. C. The role of mantle plumes in continental breakup—case histories from Gondwanaland. *Nature* **377,** 301–308 (1995).
65. Sleep, N. H., Richards, M. A. & Hager, B. H. On the onset of mantle plumes in the presence of preexisting convection. *J. Geophys. Res.* **93,** 7672–7689 (1988).
66. Davies, G. F. & Gurnis, M. Interaction of mantle dregs with convection: lateral heterogeneity at the core-mantle boundary. *Geophys. Res. Lett.* **13,** 1517–1520 (1986).
67. Sleep, N. H. Gradual entrainment of a chemical layer at the base of the mantle by overlying convection. *Geophys. J.* **95,** 437–447 (1988).
68. Goarant, F., Guyot, F., Peyronneau, J. & Poirier, J. P. High pressure and high-temperature reactions between silicates and liquid iron alloys, in the diamond anvil cell, studied by analytical electron microscopy. *J. Geophys. Res.* **97,** 4477–4487 (1992).
69. Song, Y. & Ahrens, T. J. Pressure-temperature range of reactions between liquid iron in the outer core and mantle silicates. *Geophys. Res. Lett.* **21,** 153–156 (1994).
70. Ito, E., Morooka, K., Ujike, O. & Katsura, T. Reactions between molten iron and silicate melts at high pressure: Implications for the chemical evolution of Earth's core. *J. Geophys. Res.* **100,** 5901–5910 (1995).
71. Manga, M. & Jeanloz, R. Implications of a metal-bearing chemical boundary layer in D″ for mantle dynamics. *Geophys. Res. Lett.* **23,** 3091–3094 (1996).
72. Rigden, S. M., Ahrens, T. J. & Stolper, E. M. High-pressure equation of state of molten anorthite and diopside. *J. Geophys. Res.* **94,** 9508–9522 (1989).
73. McFarlane, E., Drake, M. J. & Rubie, D. C. Element partitioning between Mg-perovskite, magnesio-wüstite and silicate melt at conditions of the Earth's mantle. *Geochim. Cosmochim. Acta* **58,** 5161–5172 (1994).
74. Ohtani, E., Kato, T. & Ito, E. Transition metal partitioning between lower mantle and core materials. *Geophys. Res. Lett.* **18,** 85–88 (1991).
75. Duffy, T. & Ahrens, T. J. in *High-Pressure Research: Application to Earth and Planetary Sciences* (eds Syono, Y. & Manghnani, M. H.) 197–205 (Terra Scientific, Tokyo, 1992).
76. Knittle, E. The solid/liquid partitioning of major and radiogenic elements at lower mantle pressures: Implications for the core-mantle boundary region. in *The Core-Mantle Boundary* (eds Gurnis, M., Buffett, B. A., Knittle, E. & Wysession, M.) (Am Geophys. Union, in the press).
77. Holland, K. G. & Ahrens, T. J. Melting of (Mg, Fe)$_2$SiO$_4$ at the core-mantle boundary of the Earth. *Science* **275,** 1623–1625 (1997).
78. Crough, S. T. & Jurdy, D. M. Subducted lithosphere, hot spots and the geoid. *Earth Planet. Sci. Lett.* **48,** 15–22 (1980).
79. Karato, S. I., Zhang, S. & Wenk, H. R. Superplasticity in Earth's lower mantle: Evidence from seismic anisotropy and rock physics. *Science* **270,** 458–461 (1995).
80. Frost, H. J. & Ashby, M. F. *Deformation Mechanism Maps* (Pergamon, Oxford, 1982).
81. Cohen, R. E. in *High-Pressure Research: Application to Earth and Planetary Sciences* (eds Syono, Y. & Manghnani, M. H.) 425–431 (Terra Scientific, Tokyo, 1992).
82. Stewart, D. N., Buse, F. H., Walker, K. A. & Gubbins, D. Geomagnetism, Earth rotation and the electrical conductivity of the lower mantle. *Phys. Earth Planet. Inter.* **92,** 199–214 (1995).
83. Larson, R. L. & Olson, P. Mantle plumes control magnetic reversal frequency. *Earth Planet Sci. Lett.* **107,** 437–447 (1991).
84. Marzocchi, W. & Mulargia, F. The periodicity of geomagnetic reversals. *Phys. Earth Planet. Inter.* **73,** 222–228 (1992).
85. Laj, C., Mazaud, A., Weeks, R., Fuller, M. & Herrero-Berverra, E. Geomagnetic reversal paths. *Nature* **351,** 447–450 (1991).
86. Valet, J. P., Tucholka, P., Courtillot, V. & Meynadier, L. Palaeomagnetic constraints on the geometry of the geomagnetic field during reversals. *Nature* **356,** 400–407 (1992).
87. Hoffman, K. Dipolar reversal states of the geomagnetic field and core-mantle dynamics. *Nature* **359,** 789–794 (1992).
88. Aurnou, J. M., Buttles, J. L., Neumann, G. A. & Olson, P. L. Electromagnetic core-mantle coupling and paleomagnetic reversal paths. *Geophys. Res. Lett.* **23,** 2705–2708 (1996).
89. Courtillot, V. & Valet, J. P. Secular variation of the Earth's magnetic field: From jerks to reversals. *C. R. Acad. Sci.* **320,** 903–922 (1995).
90. Shankland, T. J., Peyronneau, J. & Poirier, J. P. Electrical conductivity of the Earth's lower mantle. *Nature* **366,** 453–455 (1993).
91. Li, X. & Jeanloz, R. Laboratory studies of the electrical conductivity of silicate perovskites at high pressures and temperatures. *J. Geophys. Res.* **95,** 5067–5078 (1990).
92. Tonks, W. B. & Melosh, H. J. in *Origin of the Earth* (eds Newsom, H. E. & Jones, J. H.) 151–174 (Oxford Univ. Press, New York, 1990).
93. Birch, F. Elasticity and constitution of the Earth's interior. *J. Geophys. Res.* **57,** 227–286 (1952).
94. Lithgow-Bertelloni, C. & Richards, M. A. The dynamics of Cenozoic and Mesozoic plate motions. *Annu. Rev. Earth Planet. Sci.* (in the press).


**Acknowledgements.** We thank C. Lithgow-Bertelloni, R. van der Hilst and S. Grand for providing access to their models and M. Kendall for providing comments on the manuscript. This work was supported by the US National Science Foundation.

Correspondence should be addressed to T.L. (e-mail: thorne@earthsci.ucsc.edu).